

DHIL-GT: Scalable Graph Transformer with Decoupled Hierarchy Labeling

Ningyi Liao*

Nanyang Technological University
Singapore
liao0090@e.ntu.edu.sg

Zihao Yu*

Nanyang Technological University
Singapore
zihao.yu@ntu.edu.sg

Siqiang Luo

Nanyang Technological University
Singapore
siqiang.luo@ntu.edu.sg

ABSTRACT

Graph Transformer (GT) has recently emerged as a promising neural network architecture for learning graph-structured data. However, its global attention mechanism with quadratic complexity concerning the graph scale prevents wider application to large graphs. While current methods attempt to enhance GT scalability by altering model architecture or encoding hierarchical graph data, our analysis reveals that these models still suffer from the computational bottleneck related to graph-scale operations. In this work, we target the GT scalability issue and propose DHIL-GT, a scalable Graph Transformer that simplifies network learning by fully decoupling the graph computation to a separate stage in advance. DHIL-GT effectively retrieves hierarchical information by exploiting the graph labeling technique, as we show that the graph label hierarchy is more informative than plain adjacency by offering global connections while promoting locality, and is particularly suitable for handling complex graph patterns such as heterophily. We further design subgraph sampling and positional encoding schemes for precomputing model input on top of graph labels in an end-to-end manner. The training stage thus favorably removes graph-related computations, leading to ideal mini-batch capability and GPU utilization. Notably, the precomputation and training processes of DHIL-GT achieve complexities *linear* to the number of graph edges and nodes, respectively. Extensive experiments demonstrate that DHIL-GT is efficient in terms of computational boost and mini-batch capability over existing scalable Graph Transformer designs on large-scale benchmarks, while achieving top-tier effectiveness on both homophilous and heterophilous graphs.

CCS CONCEPTS

• **Computing methodologies** → **Neural networks**; • **Mathematics of computing** → *Graph algorithms*.

KEYWORDS

Graph neural networks, Graph Transformer, Scalable computation

1 INTRODUCTION

Graph Transformers characterize a family of neural networks that introduce the powerful Transformer architecture [33] to the realm of graph data learning. These models have garnered increasing research interest due to their unique applications and competitive performance [18, 39, 41, 46]. Despite their achievements, vanilla GTs are highly limited to specific tasks because of the full-graph attention mechanism, which has computational complexity at least quadratic to the graph size, rendering it impractical for a single

graph with more than thousands of nodes. Enhancing the scalability of GTs is thus a prominent task for enabling these models to handle a wider range of graph data on large scales.

To scale up Graph Transformers, existing studies explore various strategies to retrieve and utilize graph data efficiently. One representative approach is to simplify the model architecture with a specialized attention module [30, 37, 38]. The graph topology is conserved by the message-passing mechanism, which recognizes edge connections without the need for quadratic computation on all-pair node interactions. However, these modifications introduce another computational bottleneck of iterative graph propagation, which typically has an overhead linear to the edge size and remains challenging for scalable model training. An alternative line of works chooses to embed richer topological information as structured data through different graph processing techniques, such as adjacency-based spatial propagation [7, 21], polynomial spectral transformation [12, 27], and hierarchical graph coarsening [42, 45]. Although these models offer a relatively scalable model training scheme, the graph-related operation still persists during their learning pipeline, leaving certain scalability and expressivity issues unsolved as detailed in our complexity analysis.

In this work, we propose DHIL-GT, a scalable Graph Transformer with Decoupled Hierarchy Labeling. By constructing a hierarchical graph label set consisting of node pair connections and distances, we showcase that all graph information necessary for GT learning can be fully decoupled and produced by an end-to-end pipeline before training. The precomputation procedure can be finished within a linear $O(m)$ bound, while the iterative learning step is as simple as training normal Transformers with $O(n)$ complexity, where m and n are the numbers of graph edges and nodes, respectively. The two stages achieve theoretical complexities on par with respective state-of-the-art GTs, as well as a substantial boost in practice thanks to empirical acceleration strategies.

Our DHIL-GT is based on the 2-hop labeling technique, which has been extensively studied with scalable algorithms for querying the shortest path distance (SPD) between nodes [1, 2, 40]. By investigating its properties, we show that the graph labels construct a hierarchical representation of the graph topology, favorably containing both local and global graph connections. We design a novel subgraph token generation process to utilize the labels as informative input for GT. The data hierarchy benefits GT expressivity in modeling node-pair interactions beyond graph edges, which is superior in capturing graph knowledge under both homophily and heterophily compared to current locality-based GTs. In addition, the built graph labels also offer a simple and fast approach to query pair-wise distance as positional encoding. To this end, graph information is decently embedded into the precomputed data from

*Both authors contributed equally to this research.

Table 1: Time and memory complexity of different types of Graph Transformer models with respect to precomputation and training stages. “FB”, “NS”, and “RS” refer to full-batch, neighborhood sampling, and random sampling strategies, respectively. Training time complexity represent the forward-passing computational operations on respective node sets, while precomputation complexity indicates one-time processing such as positional encoding and token generation. RAM memory represents the primary data used as input, and GPU memory is for variable graph or batch representations during learning. “Hetero” column marks whether the model evaluates data under heterophily in the original literature.

Taxonomy	Batch	Model	Precompute Time	Train Time	RAM Mem.	GPU Mem.	Hetero
Vanilla	FB	Graphormer [41]	$O(n^3)$	$O(Ln^2F)$	$O(n^2)$	$O(Ln^2F)$	N
		GRPE [29]	$O(n^2)$	$O(Ln^2F)$	$O(n^2)$	$O(Ln^2F)$	N
Kernel-based	NS	GraphGPS [30]	$O(n^3)$	$O(LnF^2 + LmF)$	$O(nF + n^2)$	$O(Ln_bF + m)$	Y
		NodeFormer [38]	–	$O(LnF^2 + LmF)$	$O(nF + m)$	$O(Ln_bF + m)$	Y
		DIFFormer [37]	–	$O(LnF^2 + LmF)$	$O(nF + m)$	$O(Ln_bF + m)$	N
		PolyNormer [12]	–	$O(LnF^2 + LmF)$	$O(nF + m)$	$O(Ln_bF + m)$	Y
Hierarchical	RS	NAGphormer [7]	$O(LmF_0)$	$O(LnF^2)$	$O(LnF)$	$O(Ln_bF^2)$	N
		PolyFormer [27]	$O(LmF_0)$	$O(LnF^2)$	$O(LnF)$	$O(Ln_bF^2)$	Y
		ANS-GT [42]	$O(ns^2 + Lm)$	$O(LnF^2 + Lns^2F +)$	$O(nF + ns^2)$	$O(Ln_bF + n_b s^2)$	Y
		GOAT [21]	$O(nF)$	$O(LnF^2 + LmF)$	$O(nF + m)$	$O(Ln_b^2 + Ln_bF + m)$	Y
		HSGT [45]	$O(n + Lm)$	$O(LnF^2 + LmF)$	$O(nF + Lm)$	$O(Ln_b^2 + Ln_bF + Lm)$	N
		DHIL-GT (ours)	$O(ns^3 + ms)$	$O(LnF^2 + Lns^2F)$	$O(nF + ns^2)$	$O(Ln_bF + n_b s^2)$	Y

different perspectives, and all computations concerning graph labels can be performed in a one-time manner with efficient implementation. The GT training stage only learns from the structured input data, which enjoys ideal scalability, including a simple mini-batch scheme and memory overhead free from the graph size.

We summarize the contributions of this work as follows:

- We propose DHIL-GT as a scalable Graph Transformer with decoupled graph computation and simple model training independent of graph operations. Both precomputation and learning stages achieve complexities only *linear* to the graph scale.
- We introduce an end-to-end precomputation pipeline for DHIL-GT based on graph labeling, efficiently embedding graph information with informative hierarchy. Dedicated token generation, positional encoding, and model architectures are designed for representing hierarchical data at multiple levels.
- We conduct comprehensive experiments to evaluate the effectiveness and efficiency of DHIL-GT against current Graph Transformers across large-scale homophilous and heterophilous graphs. DHIL-GT achieves top-tier accuracy and demonstrates competitive scalability regarding time and memory overhead.

2 RELATED WORKS

Vanilla Graph Transformers. Early GTs [14, 39, 41] are mainly proposed for graph-level learning tasks, typically involving small-scale graphs of less than a thousand nodes. Following the vanilla design, a wide range of positional encoding schemes have been invoked to the self-attention module to encode graph topology information, including graph proximity [5, 41, 42], Laplacian eigenvectors [14, 18, 22], and shortest path distance [6, 29, 43].

As listed in Table 1, the critical scalability bottleneck of these models lies in the straight-forward attention mechanism calculating all node-pair interactions in the graph, resulting $O(n^2)$ complexity of both training time and memory. If there is positional encoding,

additional preprocessing is also demanded with $O(n^2)$ or even higher overhead. A naive solution is to randomly sample a subset of nodes and adopt mini-batch learning. However, it largely overlooks graph information and results in suboptimal performance.

Kernel-based Graph Transformers. Kernelization is the method for modeling node-pair relations and replacing the vanilla self-attention scheme. For instance, NodeFormer [38] employs a kernel function based on random features, and GraphGPS [30] opts to incorporate topological representation. More expressive kernels are also developed, invoking depictions such as graph diffusion [37] and node permutation [12].

Although kernelized GTs prevent the quadratic complexity, the nature of the kernel indicates that graph data needs to be iteratively accessed during learning, which is represented by the $O(LmF)$ learning overhead in Table 1. When the graph scale is large, this term becomes dominant since the edge size m is significantly larger than the node size n . Hence, we argue that such a design is not sufficiently scalable. Another under-explored issue is the expressiveness of the neighborhood sampling (NS) strategy for forming node batches in kernel-based GTs. Similar to convolutional GNNs, NS is known to be subject to performance loss on complex graph signals due to its inductive bias on graph homophily [3, 44].

Hierarchical Graph Transformers. Recent advances reveal that it is possible to remove the full-graph attention and exploit the power of GTs to learn the latent node relations during learning. This is achieved by providing sufficient hierarchical context as input data with node-level identity. The key of this approach is crafting an effective embedding scheme to comply with GT expressivity. To realize this, NAGphormer [7], PolyFormer [27], and GOAT [21] look into representative features using adjacency propagation, spectral graph transformation, and feature space projection, respectively. ANS-GT [42] builds graph hierarchy by adaptive graph sampling

concerning subgraphs of size s , while HSGT [45] leverages graph coarsening algorithms.

Hierarchical GTs are applicable to mini-batching with random sampling (RS) as long as their graph embeddings are permutation invariant. Furthermore, since graph processing is independent of GT attention, it can be adequately improved with better algorithmic scalability. In most scenarios, the graph can be processed in $O(m)$ complexity in precomputation as shown in Table 1. Nonetheless, we note that hierarchical models, except for NAGphormer and PolyFormer, still involve graph-level operations during training, which hinders GPU utilization and causes additional overhead.

Scalable Convolutional GNNs. The scalability issue has also been extensively examined for Graph Neural Networks (GNNs) exploiting graph convolutions [19, 34]. Similar to hierarchical GTs, decoupled models propose to separate the graph computation from iterative convolution and employ dedicated acceleration, exhibiting excellent scalability on some of the largest datasets with linear or even sub-linear complexity [9, 20, 25, 36]. It is also demonstrated that such strategy is capable of handling heterophily [23, 24, 35]. Graph simplification techniques including graph sampling [8, 10, 15, 47] and coarsening [4, 13, 17] approaches are also explored for reducing the graph scale at different hierarchy levels. Although the high-level idea of scaling up convolutional GNNs is helpful towards scalable GTs, Transformer-based models are unique in respect to their graph data utilization and architectural bottlenecks, and hence require specific designs for addressing their scalability issues.

3 PRELIMINARIES

Graph Labeling. Consider a connected graph $\mathcal{G} = \langle \mathcal{V}, \mathcal{E} \rangle$ with $n = |\mathcal{V}|$ nodes and $m = |\mathcal{E}|$ edges. The node attribute matrix is $X \in \mathbb{R}^{n \times F_0}$, where F_0 is the dimension of input attributes. The neighborhood of a node v is $\mathcal{N}(v) = \{u | (v, u) \in \mathcal{E}\}$, and its degree $d(v) = |\mathcal{N}(v)|$. $\mathcal{P}(u, v)$ denotes a path from node u to v , and the shortest distance $b(u, v)$ is achieved by the path with least nodes.

The graph labeling process assigns a label $\mathcal{L}(v)$ to each node $v \in \mathcal{V}$, which is a set of pairs (u, δ) containing certain nodes u and corresponding shortest distances $\delta = b(u, v)$ between the node pairs. The graph labels compose a 2-hop cover [11] of \mathcal{G} if for an arbitrary node pair $u, v \in \mathcal{V}$, there exists $w \in \mathcal{L}(u), w \in \mathcal{L}(v)$ and $b(u, v) = b(u, w) + b(w, v)$. Given an order of all nodes in \mathcal{V} , we denote each node by a unique index $1, \dots, n$ and use $u < v$ to indicate that node u precedes node v in the sequence.

Transformer Architecture. A Transformer layer [33] projects the input representation matrix $H \in \mathbb{R}^{n \times F}$ into three subspaces:

$$Q = HW_Q, \quad K = HW_K, \quad V = HW_V, \quad (1)$$

where $W_Q \in \mathbb{R}^{F \times d_K}, W_K \in \mathbb{R}^{F \times d_K}, W_V \in \mathbb{R}^{F \times d_V}$ are the projection matrices. For a multi-head self-attention module with N_H heads, each attention head possesses its own representations $Q_i, K_i, V_i, i = 1, \dots, N_H$, and the output \tilde{H} across all heads is calculated as:

$$\tilde{H}_i = \text{softmax} \left(\frac{Q_i K_i^\top}{\sqrt{d_K}} \right) V_i, \quad \tilde{H} = (\tilde{H}_1 \| \dots \| \tilde{H}_{N_H}) W_O, \quad (2)$$

where $\cdot \| \cdot$ denotes the matrix concatenation operation. In this paper, we set the projection dimension $d_K = d_V = F/N_H$. It can be

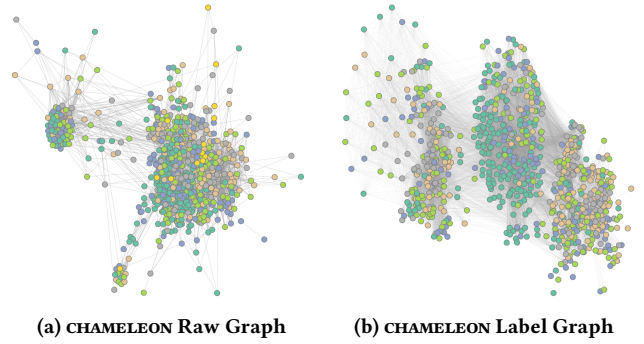


Figure 1: Visualization of the hierarchy of (a) the original graph \mathcal{G} and (b) the label graph $\hat{\mathcal{G}}$ on the heterophilous dataset CHAMELEON. Color of each node denotes its class.

observed that Eqs. (1) and (2) for representations of n nodes lead to $O(n^2 F)$ time and memory overhead. When it only applies to a batch of n_b nodes, the complexity is drastically reduced to $O(n_b^2 F)$.

4 HIERARCHY OF LABEL GRAPH

Our DHIL-GT aims to retrieve graph hierarchy information from graph labels consisting of node pair connections and distances. In this section, we first introduce the pruned landmark labeling algorithm to efficiently compute graph labels as a 2-hop cover. Then, we analyze that the labeling process favorably builds a graph hierarchy with several useful properties for representing implicit graph information beyond adjacency.

4.1 Pruned Landmark Labeling

Based on the concept of graph labeling in Section 3, a straightforward approach to build the graph labels is to traverse the whole graph for each node successively. This is, however, prohibitive due to the repetitive graph traversal procedure. Hence, we employ the Pruned Landmark Labeling (PLL) algorithm [2], which constructs labels with a more efficient search space.

The PLL algorithm is presented in Algorithm 1. It performs a pruned BFS for each node indexed 1 to n following the given order. The algorithm is agnostic to the specific search order. In this work, we follow [2] to adopt the descending order of node degrees for its satisfying performance while leaving other schemes for future exploration.

The PLL is more efficient than full-graph traversal as it prevents the visit to nodes u that have been accessed and labeled with a shorter distance $b(u, v)$ to the current source node. Intuitively, during the early rounds of pruned BFS starting from nodes v with smaller indices, the traversal is less pruned and can reach a large portion of the graph. These nodes are regarded as landmarks with higher significance and are able to appear in a large number of node labels $\mathcal{L}(u)$ where $u > v$ along with the distance information. On the contrary, for latter nodes with higher indices, the pruned traversal constrains the visit to the local neighborhood.

Thus, we reckon that the PLL process naturally builds a hierarchy embedded in the node labels. An exemplary illustration of a real-world graph is displayed in Figure 1. The original CHAMELEON graph is heterophilous, i.e., connected nodes frequently belong

to distinct classes. In Figure 1(a), different classes are mixed in graph clusters, which pose a challenge for GTs to perform classification based on edge connections. In contrast, nodes in the graph marked by graph labels in Figure 1(b) clearly form multiple densely connected clusters, exhibiting a distinct hierarchy. Certain classes can be intuitively identified from the hierarchy, which empirically demonstrates the effectiveness of our utilization of graph labeling.

4.2 Label Graph Properties

Then, we formulate the hierarchy in graph labels by defining a generated graph, namely the *label graph*, as $\hat{\mathcal{G}} = \langle \mathcal{V}, \hat{\mathcal{E}} \rangle$, which is with directed and weighted edges. Its edge set depicts the elements in node labels computed by graph labeling, that an edge $(u, v) \in \hat{\mathcal{E}}$ if and only if $(v, \delta) \in \mathcal{L}(u)$, and the edge weight is exactly the distance in graph labels $\delta = b(u, v)$. The in- and out-neighborhoods based on edge directions are $N_{in}(v) = \{u | (u, v) \in \hat{\mathcal{E}}\}$ and $N_{out}(v) = \{u | (v, u) \in \hat{\mathcal{E}}\}$, respectively.

We then elaborate the following three hierarchical properties of the label graph generated by Algorithm 1. Corresponding running examples are given in Figure 2. For simplicity, we assume that the original graph \mathcal{G} is undirected, while properties for a directed \mathcal{G} can be acquired by separately considering two label sets \mathcal{L}_{in} and \mathcal{L}_{out} for in- and out-edges in \mathcal{E} .

PROPERTY 1. For an edge $(u, v) \in \mathcal{E}$, there is $(v, u) \in \hat{\mathcal{E}}$ when $u < v$, and $(u, v) \in \hat{\mathcal{E}}$ when $u > v$.

Referring to Algorithm 1, when the current node is v and $v < u$, $\delta = 1$ holds since u is the direct neighbor of v . Hence, $(v, 1)$ is added to label $\mathcal{L}(u)$ at this round, which is equivalent to adding edge (u, v) to $\hat{\mathcal{E}}$. Similarly, $(v, u) \in \hat{\mathcal{E}}$ holds when $v > u$. For example, the edge $(1, 4)$ in Figure 2(a) is represented by the directed edge $(4, 1)$ in Figure 2(b). Property 1 implies that $N(v) \subset N_{in}(v) \cup N_{out}(v)$, i.e., the neighborhood of the original graph is also included in the label graph, and is further separated into two sets according to the relative order of neighboring nodes.

PROPERTY 2. For a shortest path $\mathcal{P}(u, v)$ in \mathcal{G} , there is $(w, v) \in \hat{\mathcal{E}}$ for each $w \in \mathcal{P}(u, v)$ satisfying $w > v$.

Algorithm 1: Pruned Landmark Labeling [2]

Input: Graph $\mathcal{G} = \langle \mathcal{V}, \mathcal{E} \rangle$

Output: Labels for all nodes \mathcal{L}

```

1 Sort  $\mathcal{V}$  based on degree  $d(v)$ 
2  $\mathcal{L}(v) \leftarrow \emptyset$  for all  $v \in \mathcal{V}$ 
3 for  $v = 1$  to  $n$  do
4   Queue  $Q \leftarrow \{(v, 0)\}$ 
5   while  $Q \neq \emptyset$  do
6     Pop the first element  $(u, \delta)$  from  $Q$ 
7      $b(u, v) \leftarrow \min\{b(u, w) + b(w, v) \mid w \in \mathcal{L}(u) \cap \mathcal{L}(v)\}$ 
8     if  $\delta < b(u, v)$  then
9        $\mathcal{L}(u) \leftarrow \mathcal{L}(u) \cup (v, \delta)$ 
10      for all  $w \in N(u)$  such that  $w > v$  do
11        Push  $(w, \delta + 1)$  to the end of  $Q$ 
12 return  $\{\mathcal{L}(v) \mid v \in \mathcal{V}\}$  as  $\mathcal{L}$ 
```

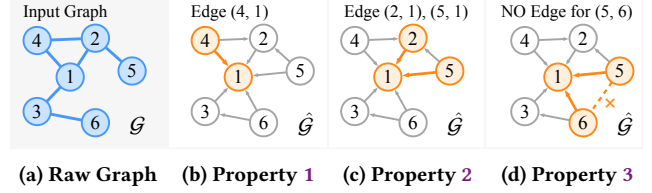


Figure 2: Examples of three properties of the label graph $\hat{\mathcal{G}}$ corresponding to the original graph \mathcal{G} . Number inside each node denotes its index in descending order of node degrees.

[2] proves that there is $v \in \mathcal{L}(w)$ for $w \in \mathcal{P}(u, v)$ and $w > v$. Therefore, considering shortest paths starting with node v of a small index, i.e., v being a “landmark” node, then succeeding nodes $w > v$ in the path are connected to v in $\hat{\mathcal{G}}$. In Figure 2(a), the shortest path between $(1, 5)$ passing node 2 results in edges $(2, 1)$ and $(5, 1)$ in Figure 2(c), since nodes 2 and 5 are in the path and their indices are larger than node 1. When the order is determined by node degree, high-degree nodes appear in shortest paths more frequently, and consequently link to a majority of nodes, including those long-tailed low-degree nodes in $\hat{\mathcal{G}}$.

PROPERTY 3. For a shortest path $\mathcal{P}(u, v)$ in \mathcal{G} , if there is $w \in \mathcal{P}(u, v)$ and $w < v$, then $(u, v) \notin \hat{\mathcal{E}}$.

According to the property of shortest path, there is $b(u, v) = b(u, w) + b(w, v)$. Hence, the condition of line 8 in Algorithm 1 is not met at the v -th round when visiting w . In other words, the traversal from v is pruned at the preceding node w . By this means, the in-neighborhood $N_{in}(v)$ is limited in the local subgraph with shortest paths ending at landmarks. As shown in Figure 2(d), the shortest path between $(5, 6)$ passes node 1, indicating that $(5, 6)$ are not directly connected since their distance can be acquired by edges $(5, 1)$ and $(6, 1)$. As a consequence, the neighborhood of node 5 in $\hat{\mathcal{G}}$ is constrained by nodes 1 and 2, preventing connections to more distant nodes such as 3 or 6.

Summarizing Properties 1 to 3, the label graph preserves neighboring connections of the original graph, while establishing more connections to a minority set of global nodes as landmark. The hierarchy is built so that long-tailed nodes with high indices are usually located in local substructures separated by landmarks. Noticeably, since the label graph is deterministic, it can be computed by Algorithm 1 in an individual stage in one time and used throughout graph learning iterations.

5 METHODOLOGY

In this section, we describe the design motivation and approach of the DHIL-GT model by respectively elaborating on the proposed modules in its precomputation and learning stages. Figure 3 illustrates the overview of the DHIL-GT pipeline.

5.1 Subgraph Generation by Labeling

Motivation: Hierarchical GT beyond adjacency. Canonical Graph Transformer models [7, 30, 38, 41] generally utilize graph adjacency for composing the input sequence in graph representation learning. However, recent advances reveal that adjacency alone is insufficient to represent the implicit graph topology. GTs

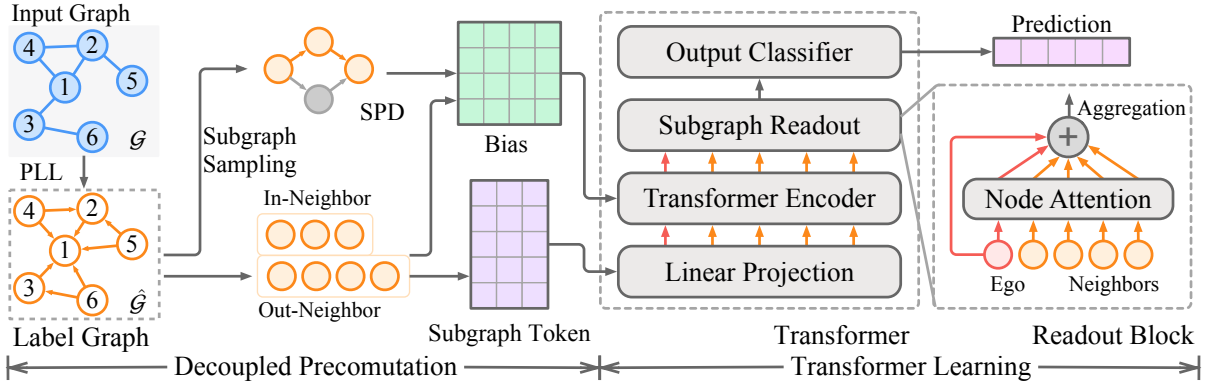


Figure 3: High-level framework of DHIL-GT including two consecutive stages of precomputation and Transformer learning. The precomputation stage processes input graph into the label graph, which is then used to generate the subgraph structure and SPD bias. During training, the subgraph tokens are applied as input features for each node, while SPD is regarded as positional encoding for Transformer layers. A readout block aggregates the subgraph representation to the ego node for prediction.

can be improved by modeling node connections not limited to explicit edges, and more hierarchical information benefits learning high-level knowledge on graph data [21, 42, 45].

Unlike existing hierarchical GTs relying on the original graph \mathcal{G} , we seek to retrieve structural information from the label graph $\hat{\mathcal{G}}$ generated by Algorithm 1. As showcased in Section 4, the label graph hierarchy processes properties of maintaining local neighborhoods while adding global edges. This is preferable for Graph Transformers as it extends the receptive field beyond local neighbors described by graph adjacency and highlights those distant but important landmarks in the graph for attention modules on node connections. The hierarchical information is especially useful for complicated scenarios, such as heterophilous graphs, where the local graph topology may be distributive or even misleading. Moreover, the edge weight of the label graph, i.e., the shortest distance between node pairs of interest, can serve as a straightforward metric for evaluating relevance with the ego node.

Algorithm 2: DHIL-GT Precomputation

Input: Graph $\mathcal{G} = \langle \mathcal{V}, \mathcal{E} \rangle$, Sample size s_{in}, s_{out} , Sampling exponents r_{in}, r_{out}

Output: Subgraphs for all nodes $\{\mathcal{S}(v)\}$, Extended edge set $\hat{\mathcal{E}}$

```

1  $\hat{\mathcal{E}} \leftarrow \emptyset$ 
2 Compute  $\mathcal{L}$  using Algorithm 1
3 for  $v = 1$  to  $n$  do
4   Add  $(v, u, \delta)$  to  $\hat{\mathcal{E}}$  for all  $(u, \delta) \in \mathcal{L}(v)$ 
5    $\mathcal{N}_{in} \leftarrow \{(u, \delta^{r_{in}}) \mid (u, \delta) \in \mathcal{L}(u)\}$ 
6    $\mathcal{N}_{out} \leftarrow \{(u, \delta^{r_{out}}) \mid (u, \delta) \in \mathcal{L}(v)\}$ 
7   Sample  $s_{in}$  nodes from  $\mathcal{N}_{in}$  with weights  $\delta^{r_{in}}$  as  $\mathcal{S}_{in}$ 
8   Sample  $s_{out}$  nodes from  $\mathcal{N}_{out}$  with weights  $\delta^{r_{out}}$  as  $\mathcal{S}_{out}$ 
9    $\mathcal{S}(v) \leftarrow \{v\} \cup \mathcal{S}_{in} \cup \mathcal{S}_{out}$ 
10  for all  $(u, w)$  such that  $u \in \mathcal{S}(v), w \in \mathcal{S}(v)$  do
11    Compute  $b(u, w)$  using Eq. (3)
12    Add  $(u, w, b(u, w))$  to  $\hat{\mathcal{E}}$ 
13 return  $\{\mathcal{S}(v) \mid v \in \mathcal{V}\}$  and  $\hat{\mathcal{E}}$ 

```

To leverage the label graph efficiently, we employ a decoupling scheme to prepare the labels and necessary data in a separate stage before training. The graph data is only processed in this precomputation stage and is prevented from being fully loaded onto GPU devices, which intrinsically reduces the GPU memory overhead and offers better scalability to large graphs.

Sampling for Subgraph Tokens. Algorithm 2 describes the precomputation process in DHIL-GT. Given the input graph \mathcal{G} , we first build the graph labels by PLL as outlined in Algorithm 1. For each node, we generate a token for GT learning, which represents the neighborhood around the node in the label graph $\hat{\mathcal{G}}$. Since the neighborhood size is variable, we convert it into a fixed-length subgraph token $\mathcal{S}(v)$ with s nodes by weighted sampling, as shown in lines 4-9 in Algorithm 2. Neighbors in $\mathcal{N}_{in}(v)$ and $\mathcal{N}_{out}(v)$ are sampled separately with different sizes, as Section 4.2 shows that these two sets contain nodes of differing importance. The distance to the ego node $b(u, v)$ is used as the sampling weight, with hyperparameters $r_{in}, r_{out} \in \mathbb{R}$ controlling the relative importance. Note that under our sampling scheme, nodes not connected to the ego node will not appear in the token.

Overall, the subgraph generation process produces a node list of length $s = s_{in} + s_{out} + 1$ for each node, representing its neighborhood in the label graph $\hat{\mathcal{G}}$. The relative values of hyperparameters s_{in} and s_{out} can be used to balance the ratio of in-neighbors and out-neighbors in $\hat{\mathcal{G}}$, which correspond to local long-tailed nodes and distant landmark nodes in \mathcal{G} , respectively. Compared to canonical GT tokens representing the graph node in the context of the full graph, DHIL-GT only relies on a small but informative subgraph of fixed size s . When the graph scales up, DHIL-GT enjoys better scalability as its token size does not increase with the graph size.

5.2 Fast Subgraph Positional Encoding

Positional encoding is critical for GT expressivity to model inter-node relationship for graph learning. In our approach, positional encoding provides the relative identity of nodes within the subgraph hierarchy. We particularly employ shortest path distance (SPD) to

token nodes as the positional encoding scheme in DHIL-GT, which is superior as it holds meaningful values for arbitrary node pairs regardless of locality. In comparison, other approaches such as graph proximity and eigenvectors are usually too sparse to provide identifiable information within sampled subgraphs.

Conventionally, calculating SPD for positional encoding demands $O(n^2)$ or higher complexity as analyzed in Table 1, which is not practical for large-scale scenarios. Thanks to the graph labeling computation, we are able to efficiently acquire SPD inside subgraphs. Recalling the definition of 2-hop cover in Section 3, we exploit the following corollary, which ensures the SPD of any node pairs can be effectively acquired on top of PLL labels:

COROLLARY 4 ([2]). *For any node pair (u, v) , the shortest path distance can be calculated by:*

$$b(u, v) = \min \{b(u, w) + b(w, v) \mid w \in \mathcal{L}(u), w \in \mathcal{L}(v)\}, \quad (3)$$

where labels \mathcal{L} are computed by Algorithm 1. Note that $b(u, v) = 0$.

The second part of Algorithm 2 in line 10-12 depicts the process of further reusing the label graph data structure for managing SPD within node-wise subgraphs. For node pairs of each subgraph $\mathcal{S}(v)$, the SPDs are computed and stored as weighted edges that extend the label graph edge set $\hat{\mathcal{E}}$.

To employ SPD positional encoding, the transformer layer in Eq. (2) is altered with a bias term $\mathbf{B} \in \mathbb{R}^{s \times s}$:

$$\tilde{\mathbf{H}} = \text{softmax} \left(\frac{\mathbf{Q}\mathbf{K}^\top}{\sqrt{d_K}} + \mathbf{B} \right) \mathbf{V}, \quad (4)$$

where the value of bias entry is a learnable parameter indexed by the node-pair SPD value $\mathbf{B}[u, v] = f_B(b(u, v))$, $f_B: \mathbb{N} \rightarrow \mathbb{R}$.

5.3 Model Architecture

DHIL-GT enhances the GT architecture [41, 42] to fit the precomputed subgraphs and mini-batch training for large-scale representation learning. Apart from the SPD bias, we also design specific modules to adapt to subgraph hierarchical learning. For each node $v \in \mathcal{V}$, given the subgraph $\mathcal{S}(v)$ produced by Algorithm 2, input representations are retrieved from the node attributes based on the input node token as $\mathbf{H}^{(0)} = \text{MLP}_X(\mathbf{X}[\mathcal{S}(v)])$, where $\mathbf{X}[\mathcal{S}(v)]$ denotes node attributes $\mathbf{X}[u]$ for all $u \in \mathcal{S}(v)$, and $\text{MLP}_X: \mathbb{R}^{s \times F_0} \rightarrow \mathbb{R}^{s \times F}$ with hidden dimension F .

For the l -th Transformer layer, the representation is updated as:

$$\begin{aligned} \tilde{\mathbf{H}}^{(l-1)} &= \text{MHA} \left(\text{LN} \left(\mathbf{H}^{(l-1)} \right) \right) + \mathbf{H}^{(l-1)}, \\ \mathbf{H}^{(l)} &= \text{FFN} \left(\text{LN} \left(\tilde{\mathbf{H}}^{(l-1)} \right) \right) + \tilde{\mathbf{H}}^{(l-1)}, \end{aligned} \quad (5)$$

where LN and FFN stand for layer normalization and feed-forward network, respectively, and MHA denotes the multi-head self-attention architecture described by Eqs. (1), (2) and (4).

Lastly, a readout layer calculates node-wise attention over the L -layer representation among nodes in the fixed-length token $\mathcal{S}(v)$:

$$\alpha_u = \frac{\exp \left((\mathbf{H}^{(L)}[v] \parallel \mathbf{H}^{(L)}[u]) \mathbf{W}_E \right)}{\sum_{u \in \mathcal{S}(v)} \exp \left((\mathbf{H}^{(L)}[v] \parallel \mathbf{H}^{(L)}[u]) \mathbf{W}_E \right)}, \quad (6)$$

which measures the correlation between ego node and its neighbors in the subgraph. The representation is then aggregated to the ego

node v as output:

$$\mathbf{Z} = \text{MLP}_Z \left(\mathbf{H}^{(L)}[v] + \sum_{u \in \mathcal{S}(v)} \alpha_u \mathbf{H}^{(L)}[u] \right), \quad (7)$$

where MLP_Z is the output classifier.

Virtual Node. We add virtual nodes representing landmarks to $\hat{\mathcal{G}}$ such that $(0, v) \in \hat{\mathcal{E}}$, $b(0, v) = \infty$ for all nodes $v \in \mathcal{V}$. It can be observed from Algorithm 1 that virtual nodes are added to every $\mathcal{S}(v)$ without affecting label construction and SPD query. During the learning stage, we set their attributes and attention bias to be learnable. This scheme actually generalizes the global virtual node utilized in [41], offering graph-level context to node-level representation during representation updates.

Mini-batch Capability. Remarkably, throughout the Transformer learning stage of DHIL-GT, input data including subgraph tokens, SPD bias, and node attributes are all readily prepared by Algorithm 2 as described in previous subsections. For each node, only indexing operations are performed on \mathbf{X} and $\hat{\mathcal{E}}$ based on the subgraph token $\mathcal{S}(v)$, and no graph-scale computation is required during learning iterations. Therefore, mini-batch training for DHIL-GT can be easily implemented by sampling batches of ego nodes, and only indexed strides of \mathbf{X} and $\hat{\mathcal{E}}$ are loaded onto GPU devices.

5.4 Complexity Analysis

To characterize the model scalability, we consider the time and memory complexity of DHIL-GT separately in the precomputation and learning stages. In precomputation, the PLL labeling and sampling process Algorithm 1 satisfies the analysis in [2], entailing a complexity of $O(ns + ms)$ for computing labels of all nodes. Regarding the positional encoding, a single SPD query following Corollary 4 can be calculated in $O(s)$ time within the subgraph. The query is performed at most $O(ns^2)$ times for all nodes, which leads to an $O(ns^3)$ overhead for $\hat{\mathcal{E}}$ in total. It is worth noting that the empirical number of queries is significantly smaller than the above bound, since the subgraphs $\mathcal{S}(v)$ are highly overlapped for neighboring nodes. The memory overhead for managing sampled tokens and features in RAM is $O(ns^2)$ and $O(nF)$, respectively. Note that SPD values are stored as integers, which is more efficient than other positional encoding schemes.

During model training, one epoch of L -layer feature transformation on all nodes demands $O(LnF)$ operations, while bias projection is performed with $O(ns^2)$ time complexity. The GPU memory footprint for handling a batch of node representations and bias matrices is $O(Ln_bF)$ and $n_b s^2$, respectively, where n_b is the batch size. It can be observed that the training overhead is only determined by batch size and is free from the graph scale, ensuring favorable scalability for iterative GT updates.

6 EXPERIMENTS

We comprehensively evaluate the performance of DHIL-GT with a wide range of datasets and baselines. In Section 6.2, we highlight the model efficiency regarding time and memory overhead, as well as its effectiveness under both homophily and heterophily. Sections 6.3 and 6.4 provides in-depth insights into the effect of

Table 2: Effectiveness and efficiency results on heterophilous datasets, while evaluation on homophilous datasets are in Table 4. “Pre.”, “Epoch”, and “Infer” are precomputation, training epoch, and inference time (in seconds), respectively. “Mem.” refers to peak GPU memory throughout the whole learning process (GB). Respective results of the first and second best performances in each dataset are marked in bold and underlined fonts.

Small	CHAMELEON					SQUIRREL					TOLOKERS				
	Pre.	Epoch	Infer	Mem.	Acc	Pre.	Epoch	Infer	Mem.	Acc	Pre.	Epoch	Infer	Mem.	ROC AUC
DIFFormer*	-	0.09	0.38	0.50	37.83±4.54	-	0.05	0.05	0.7	35.73±1.37	-	0.16	85.8	0.88	74.88±0.59
PolyNormer*	-	0.03	0.17	1.1	40.70±3.38	-	0.07	0.49	1.2	38.40 ±1.10	-	1.27	15.5	9.4	79.39±0.50
NAGphormer	0.27	0.03	0.03	0.5	33.18±4.30	0.85	0.08	0.08	0.5	32.02±3.93	1.59	0.11	0.02	0.5	79.32±0.39
ANS-GT	11.2	1.98	0.78	2.8	<u>41.19</u> ±0.69	28.1	4.48	1.95	6.6	37.15±1.10	716	2.37	3.42	10.7	79.31±0.97
GOAT	1.99	0.34	0.44	0.4	35.02±1.15	6.66	0.37	0.58	0.6	30.78±0.91	36.1	5.49	5.87	5.0	<u>79.46</u> ±0.57
HSGT*	0.01	0.34	0.73	0.3	32.28±2.43	0.01	0.42	0.74	0.4	34.32±0.51	2.62	7.76	8.12	17.4	<u>79.24</u> ±0.83
DHIL-GT (ours)	0.08	0.03	0.005	4.5	43.63 ±2.34	0.35	0.68	0.01	5.7	<u>37.16</u> ±0.57	1.9	0.17	0.02	7.2	79.86 ±0.47
Large	PENN94					GENIUS					TWITCH-GAMER				
	Pre.	Epoch	Infer	Mem.	Acc	Pre.	Epoch	Infer	Mem.	Acc	Pre.	Epoch	Infer	Mem.	Acc
DIFFormer*	-	0.53	0.65	5.5	61.77±3.41	-	0.77	5.47	5.4	84.52±0.36	-	0.61	5.14	4.9	60.81±0.44
PolyNormer*	-	0.58	18.4	6.3	79.87 ±0.06	-	0.77	28	12.9	<u>85.64</u> ±0.52	-	1.45	89	21.4	<u>64.72</u> ±0.65
NAGphormer	237	6.14	2.13	2.3	74.45±0.60	38	5.43	1.04	2.3	83.88±0.13	16	1.92	0.39	2.3	61.92±0.19
ANS-GT	3889	42	4.9	8.7	67.76±1.32	34092	37	4.95	8.7	67.76±1.32	12924	19	6.7	8.6	61.55±0.45
GOAT	1332	33	18	20.9	71.42±0.44	2664	28	39	8.9	80.12±2.32	3348	37	63	21.2	61.38±0.83
HSGT*	12	115	110	9.3	67.77±0.27	21	98	114	17.1	84.03±0.24	68	235	253	11.2	61.60±0.09
DHIL-GT (ours)	31	14	0.3	10.2	<u>78.74</u> ±0.45	52	5.4	0.33	7.0	91.06 ±0.47	172	2.2	0.15	7.3	67.03 ±2.17

* Inference of these models is performed on the CPU in a full-batch manner due to their requirement of the whole graph.

DHIL-GT designs in exploiting graph hierarchy. Implementation details and full experimental results can be found in Appendix A.

6.1 Experimental Settings

Tasks and Datasets. We focus on the node classification task on 12 benchmark datasets in total covering both homophily [16, 31, 32] and heterophily [26, 28], whose statistics are listed in Table 5. Compared to conventional graph learning tasks used in GT studies, this task requires learning on large single graphs, which is suitable for assessing model scalability. We follow common data processing and evaluation protocols as detailed in Appendix A.1. Evaluation is conducted on a server with 32 Intel Xeon CPUs (2.4GHz), an Nvidia A30 GPU (24GB memory), and 512GB RAM.

Baselines. Since the scope of this work lies in the efficacy and efficiency enhancement of the GT architecture, we primarily compare against state-of-the-art Graph Transformer models with attention-based layers and mini-batch capability. Methods including DIFFormer [37] and PolyNormer [12] are considered as kernel-based approaches. NAGphormer [7], GOAT [21], HSGT [45], and ANS-GT [42] stand for hierarchical GTs.

Evaluation Metrics. We use ROC AUC as the efficacy metric on TOLOKERS and classification accuracy on the other datasets. For efficiency evaluation, we notice that there is limited consensus due to the great variety in GT training schemes. Therefore, we attempt to employ a comprehensive evaluation considering both time and memory overhead for a fair comparison. Model speed is represented by the average training time per epoch and the inference time on the testing set. For models with graph precomputation, the time

for this process is separately recorded. We also feature the GPU memory footprint, which is the scalability bottleneck.

6.2 Performance Comparison

Table 2 presents the efficacy and efficiency evaluation results on 6 heterophilous datasets, while metrics for 6 homophilous graphs can be found in Table 4. As an overview, DHIL-GT demonstrates fast computation speed and favorable mini-batch scalability throughout the learning process. It also reaches top-tier accuracy by outperforming the state-of-the-art GTs on multiple datasets.

Time Efficiency. Benefiting from the decoupled architecture, DHIL-GT is powerful in achieving competitive speed with existing efficiency-oriented GT designs. For baselines with heavy precomputation overhead, including ANS-GT and GOAT, DHIL-GT showcases speed improvements by orders of magnitude, with up to 700× boost over ANS-GT on GENIUS. Aligned with our complexity analysis in Section 2, the key impact factor of DHIL-GT is the node size n and is less affected by m and F compared to precomputation in other methods. Meanwhile, DHIL-GT is capable of performing the fastest inference even on large-scale graphs, thanks to its simple model transformation without graph-scale operations. Its training speed is also on par with the best competitors, which usually exploit highly simplified architectures. In contrast, models including PolyNormer and HSGT suffer from longer learning times due to their iterative graph extraction and transformation.

Memory Footprint. In modern computing platforms, GPU memory is usually highly constrained and becomes the scalability bottleneck for the resource-intensive graph learning. DHIL-GT exhibits efficient utilization of GPU for training with larger batch sizes while

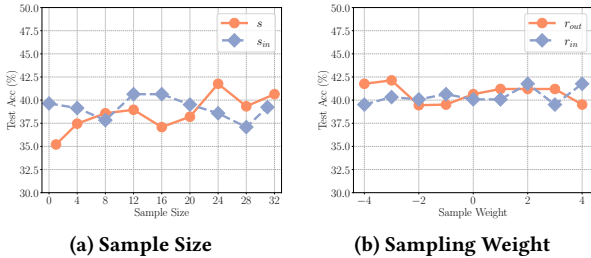


Figure 4: Effect of subgraph parameters on CHAMELEON.

avoiding the out-of-memory issue. In comparison, drawbacks in several model designs prevent them from efficiently performing GPU computation, which stems from the adoption of graph operations. Notably, kernel-based models require full graph message-passing in their inference stage, which is largely prohibitive on GPUs and can only be conducted on CPUs. HSGT faces the similar issue caused by its graph coarsening module. We note that these solutions are less scalable and hinder the GPU utilization during training. In addition, ANS-GT typically demands high memory footprint for storing and adjusting its subgraphs, which exceeds the memory limit of our platform in Table 4.

Prediction Accuracy. DHIL-GT successfully achieves significant accuracy improvement on several heterophily datasets such as CHAMELEON and TWITCH-GAMER, while the performance on other heterophilous and homophilous datasets in Tables 2 and 4 is also comparable with the state of the art. We attribute the performance gain to the application of the label graph hierarchy in DHIL-GT, which effectively addresses the heterophily issue of these graphs as analyzed in Section 4. Since the label graph also preserves edges in the raw graph, the performance of DHIL-GT is usually not lower than learning on the latter. In comparison, baseline methods without heterophily-oriented designs, including DIFformer, NAGphormer, and HSGT, perform generally worse on these graphs. This is because their models tend to rely on the raw adjacency or even promote it with higher modularity. As a consequence, node connections retrieved by GT attention modules are restrained in the local neighborhood and fail to produce accurate classifications. On the other hand, while PolyNormer achieves remarkable accuracy on several heterophilous graphs thanks to its strong expressivity, its performance is largely suboptimal on homophilous graphs in Table 4.

6.3 Effect of Hyperparameters

We then study the effectiveness of the label graph hierarchy in DHIL-GT featuring the subgraph generation process in Figure 4, which displays the impact of sample size s , s_{in} and sampling exponents r_{in} , r_{out} corresponding to Algorithm 2. Regarding the total subgraph size s , it can be observed from Figure 4(a) that a reasonably large s is essential for effectively representing graph labels and achieving stable accuracy. In the main experiments, we uniformly adopt a constant $s = 32$ token size across all datasets, as it is large enough to cover the neighborhood of most nodes while maintaining computational efficiency. As a reference, the average neighborhood size among all nodes is 16.0 on CITESEER and 31.2 on CHAMELEON. Within the fixed token length, an equal partition for

in- and out-neighbors is preferable according to Figure 4(a), where impact of s_{in} is shown when $s = 32$.

Figure 4(b) presents the result of changing the sampling weight factor. For CHAMELEON, in the plot, negative exponents favoring nodes with small SPD values are more advantageous to the model performance. Nonetheless, the variance is not significant as long as the subgraph effectively covers the neighborhood of the majority of nodes. We hence conclude that Algorithm 2 for DHIL-GT precomputation does not require precise hyperparameter tuning.

6.4 Ablation Study

Table 3 examines the respective effectiveness of the hierarchical modules in the DHIL-GT network architecture, where we separately present results on homophilous and heterophilous datasets. It can be observed that the model without SPD bias suffers the greatest accuracy drop, since topological information represented by positional encoding is necessary for GTs to retrieve the relative connection between nodes and gain performance improvement over learning plain node-level features.

In DHIL-GT, the learnable virtual node representation is invoked to provide adaptive graph-level context before Transformer layers, while the attention-based node-wise readout module aims to distinguish nodes inside subgraphs and aggregate useful representation after encoder transformation. As shown in Table 3, both modules achieve relatively higher accuracy improvements on the heterophilous graph CHAMELEON, which validates that the proposed designs are particularly suitable for addressing the heterophily issue by recognizing hierarchical information.

Table 3: Ablation study of DHIL-GT model components. The first line shows the accuracy of the complete DHIL-GT architecture. Each subsequent line indicates the performance difference when the specified module is removed.

Dataset	CITeseer	Δ	CHAMELEON	Δ
DHIL-GT	74.91	-	43.63	-
- Node Readout	72.21	-2.70	38.76	-4.87
- Virtual Node	71.15	-3.76	37.08	-6.55
- SPD Bias	68.55	-6.36	36.52	-7.11

7 CONCLUSION

In this work, we present DHIL-GT for leveraging decoupled graph hierarchy by graph labeling. Our analysis reveals that the label graph exhibits an informative hierarchy and enhances attention learning on the connections between nodes. Regarding efficiency, construction and distance query of the label graph can be accomplished with *linear* complexity and are decoupled from iterative model training. Hence, the model benefits from scalability in computation speed and mini-batch training. Empirical evaluation showcases the superiority of DHIL-GT especially under heterophily.

ACKNOWLEDGMENTS

REFERENCES

- [1] Takuya Akiba, Takanori Hayashi, Nozomi Nori, Yoichi Iwata, and Yuichi Yoshida. 2015. Efficient top-k shortest-path distance queries on large networks by pruned landmark labeling. In *Proceedings of the AAAI Conference on Artificial Intelligence*, Vol. 29.
- [2] Takuya Akiba, Yoichi Iwata, and Yuichi Yoshida. 2013. Fast exact shortest-path distance queries on large networks by pruned landmark labeling. In *Proceedings of the 2013 ACM SIGMOD International Conference on Management of Data*. ACM, 349–360. <https://doi.org/10.1145/2463676.2465315>
- [3] Adam Breuer, Roei Eilat, and Udi Weinsberg. 2020. Friend or Faux: Graph-Based Early Detection of Fake Accounts on Social Networks. In *Proceedings of The Web Conference 2020 (Taipei, Taiwan) (WWW '20)*. ACM, 1287–1297. <https://doi.org/10.1145/3366423.3380204>
- [4] Chen Cai, Dingkang Wang, and Yusu Wang. 2021. Graph Coarsening with Neural Networks. In *9th International Conference on Learning Representations*.
- [5] Cong Chen, Chaofan Tao, and Ngai Wong. 2021. Litegt: Efficient and lightweight graph transformers. In *Proceedings of the 30th ACM International Conference on Information & Knowledge Management*. 161–170.
- [6] Dexiong Chen, Leslie O’Bray, and Karsten Borgwardt. 2022. Structure-aware transformer for graph representation learning. In *International Conference on Machine Learning*. PMLR, 3469–3489.
- [7] Jinsong Chen, Kaiyuan Gao, Gaichao Li, and Kun He. 2023. NAGphormer: A Tokenized Graph Transformer for Node Classification in Large Graphs. In *11th International Conference on Learning Representations*.
- [8] Jie Chen, Tengfei Ma, and Cao Xiao. 2018. FastGCN: Fast Learning with Graph Convolutional Networks Via Importance Sampling. In *6th International Conference on Learning Representations*. 1–15.
- [9] Ming Chen, Zhewei Wei, Bolin Ding, Yaliang Li, Ye Yuan, Xiaoyong Du, and Ji Rong Wen. 2020. Scalable graph neural networks via bidirectional propagation. *33rd Advances in Neural Information Processing Systems* (2020).
- [10] Wei-Lin Chiang, Xuanqing Liu, Si Si, Yang Li, Samy Bengio, and Cho-Jui Hsieh. 2019. Cluster-gcn: An efficient algorithm for training deep and large graph convolutional networks. In *Proceedings of the 25th ACM SIGKDD International Conference on Knowledge Discovery & Data Mining*. 257–266.
- [11] Edith Cohen, Eran Halperin, Haim Kaplan, and Uri Zwick. 2003. Reachability and Distance Queries via 2-Hop Labels. *SIAM J. Comput.* 32, 5 (2003), 1338–1355. <https://doi.org/10.1137/S0097539702403098>
- [12] Chenhui Deng, Zichao Yue, and Zhiru Zhang. 2024. Polynormer: Polynomial-Expressive Graph Transformer in Linear Time. *The Twelfth International Conference on Learning Representations* (2024).
- [13] Chenhui Deng, Zhiqiang Zhao, Yongyu Wang, Zhiru Zhang, and Zhuo Feng. 2020. GraphZoom: A multi-level spectral approach for accurate and scalable graph embedding. In *8th International Conference on Learning Representations*.
- [14] Vijay Prakash Dwivedi and Xavier Bresson. 2020. A generalization of transformer networks to graphs. *arXiv preprint arXiv:2012.09699* (2020).
- [15] Wenzheng Feng, Yuxiao Dong, Tinglin Huang, Ziqi Yin, Xu Cheng, Evgeny Kharlamov, and Jie Tang. 2022. GRAND+: Scalable Graph Random Neural Networks. In *Proceedings of the ACM Web Conference 2022*. ACM, 3248–3258. [arXiv:2203.06389](https://arxiv.org/abs/2203.06389)
- [16] Weihua Hu, Matthias Fey, Marinka Zitnik, Yuxiao Dong, Hongyu Ren, Bowen Liu, Michele Catasta, Jure Leskovec, Regina Barzilay, Peter Battaglia, Yoshua Bengio, Michael Bronstein, Stephan Günnemann, Will Hamilton, Tommi Jaakkola, Stefanie Jegelka, Maximilian Nickel, Chris Re, Le Song, Jian Tang, Max Welling, and Rich Zemel. 2020. Open Graph Benchmark: Datasets for Machine Learning on Graphs. *33rd Advances in Neural Information Processing Systems* (2020).
- [17] Zengfeng Huang, Shengzhong Zhang, Chong Xi, Tang Liu, and Min Zhou. 2021. Scaling Up Graph Neural Networks Via Graph Coarsening. In *Proceedings of the 27th ACM SIGKDD Conference on Knowledge Discovery & Data Mining*, Vol. 1. ACM, Virtual Event Singapore, 675–684.
- [18] Md Shamim Hussain, Mohammed J Zaki, and Dharmashankar Subramanian. 2022. Global self-attention as a replacement for graph convolution. In *Proceedings of the 28th ACM SIGKDD Conference on Knowledge Discovery and Data Mining*. 655–665.
- [19] Thomas N Kipf and Max Welling. 2017. Semi-supervised classification with graph convolutional networks. In *International Conference on Learning Representations*.
- [20] Johannes Klicpera, Aleksandar Bojchevski, and Stephan Günnemann. 2019. Predict then propagate: Graph neural networks meet personalized PageRank. *7th International Conference on Learning Representations* (2019), 1–15.
- [21] Kezhi Kong, Jiuhai Chen, John Kirchenbauer, Renkun Ni, C Bayan Brass, and Tom Goldstein. 2023. GOAT: A global transformer on large-scale graphs. In *International Conference on Machine Learning*. PMLR, 17375–17390.
- [22] Devin Kreuzer, Dominique Beaini, Will Hamilton, Vincent Létourneau, and Prudencio Tossou. 2021. Rethinking graph transformers with spectral attention. *Advances in Neural Information Processing Systems* 34 (2021), 21618–21629.
- [23] Qimai Li, Xiaotong Zhang, Han Liu, Quanyu Dai, and Xiao-Ming Wu. 2021. Dimensionwise Separable 2-D Graph Convolution for Unsupervised and Semi-Supervised Learning on Graphs. In *Proceedings of the 27th ACM SIGKDD Conference on Knowledge Discovery & Data Mining*. ACM, Virtual Event Singapore, 953–963. <https://doi.org/10.1145/3447548.3467413>
- [24] Ningyi Liao, Siqiang Luo, Xiang Li, and Jieming Shi. 2023. LD2: Scalable Heterophilous Graph Neural Network with Decoupled Embedding. In *36th Advances in Neural Information Processing Systems*, Vol. 36. Curran Associates, Inc., 10197–10209.
- [25] Ningyi Liao, Dingheng Mo, Siqiang Luo, Xiang Li, and Pengcheng Yin. 2022. SCARA: Scalable Graph Neural Networks with Feature-Oriented Optimization. *Proceedings of the VLDB Endowment* 15, 11 (2022), 3240–3248. <https://doi.org/10.14778/3551793.3551866> [arXiv:2207.09179](https://arxiv.org/abs/2207.09179)
- [26] Derek Lim, Felix Hohne, Xiuyu Li, Sijia Linda Huang, Vaishnavi Gupta, Omkar Bhalerao, and Ser-Nam Lim. 2021. Large Scale Learning on Non-Homophilous Graphs: New Benchmarks and Strong Simple Methods. In *34th Advances in Neural Information Processing Systems*.
- [27] Jiahong Ma, Mingguo He, and Zhewei Wei. 2023. PolyFormer: Scalable Graph Transformer via Polynomial Attention. (2023).
- [28] Oleg Platonov, Denis Kuznetsov, Michael Diskin, Artem Babenko, and Liudmila Prokhorova. 2023. A Critical Look at Evaluation of GNNs under Heterophily: Are We Really Making Progress?. In *11th International Conference on Learning Representations*.
- [29] Wonpyo Park, Woong-Gi Chang, Donggeon Lee, Juntae Kim, et al. 2022. GRPE: Relative Positional Encoding for Graph Transformer. In *ICLR2022 Machine Learning for Drug Discovery*.
- [30] Ladislav Rampáček, Michael Galkin, Vijay Prakash Dwivedi, Anh Tuan Luu, Guy Wolf, and Dominique Beaini. 2022. Recipe for a general, powerful, scalable graph transformer. *Advances in Neural Information Processing Systems* 35 (2022), 14501–14515.
- [31] Prithviraj Sen, Galileo Namata, Mustafa Bilgic, Lise Getoor, Brian Galligher, and Tina Eliassi-Rad. 2008. Collective Classification in Network Data. *AI Magazine* 29, 3 (Sep. 2008), 93.
- [32] Aleksandr Shchur, Maximilian Mumme, Aleksandar Bojchevski, and Stephan Günnemann. 2018. Pitfalls of graph neural network evaluation. *arXiv preprint arXiv:1811.05868* (2018).
- [33] Ashish Vaswani, Noam Shazeer, Niki Parmar, Jakob Uszkoreit, Llion Jones, Aidan N Gomez, Łukasz Kaiser, and Illia Polosukhin. 2017. Attention is All you Need. In *Advances in Neural Information Processing Systems*, I. Guyon, U. Von Luxburg, S. Bengio, H. Wallach, R. Fergus, S. Vishwanathan, and R. Garnett (Eds.), Vol. 30. Curran Associates, Inc.
- [34] Petar Veličković, Guillem Cucurull, Arantxa Casanova, Adriana Romero, Pietro Lio, and Yoshua Bengio. 2017. Graph attention networks. In *8th International Conference on Learning Representations*.
- [35] Xiyuan Wang and Muhan Zhang. 2022. How Powerful are Spectral Graph Neural Networks. In *39th International Conference on Machine Learning*. [arXiv:2205.11172](https://arxiv.org/abs/2205.11172) [cs]
- [36] Felix Wu, Amauri Souza, Tianyi Zhang, Christopher Fifty, Tao Yu, and Kilian Weinberger. 2019. Simplifying Graph Convolutional Networks. In *Proceedings of the 36th International Conference on Machine Learning*. Kamalika Chaudhuri and Ruslan Salakhutdinov (Eds.), Vol. 97. 6861–6871.
- [37] Qitian Wu, Chenxiao Yang, Wentao Zhao, Yixuan He, David Wipf, and Junchi Yan. 2023. DIFformer: Scalable (Graph) Transformers Induced by Energy Constrained Diffusion. In *The Eleventh International Conference on Learning Representations*.
- [38] Qitian Wu, Wentao Zhao, Zenan Li, David P Wipf, and Junchi Yan. 2022. Nodeformer: A scalable graph structure learning transformer for node classification. *Advances in Neural Information Processing Systems* 35 (2022), 27387–27401.
- [39] Zhanghao Wu, Paras Jain, Matthew Wright, Azalia Mirhoseini, Joseph E Gonzalez, and Ion Stoica. 2021. Representing long-range context for graph neural networks with global attention. *Advances in Neural Information Processing Systems* 34 (2021), 13266–13279.
- [40] Yosuke Yano, Takuya Akiba, Yoichi Iwata, and Yuichi Yoshida. 2013. Fast and scalable reachability queries on graphs by pruned labeling with landmarks and paths. In *Proceedings of the 22nd ACM international conference on Information & Knowledge Management*. 1601–1606.
- [41] Chengxuan Ying, Tianle Cai, Shengjie Luo, Shuxin Zheng, Guolin Ke, Di He, Yanming Shen, and Tie-Yan Liu. 2021. Do transformers really perform badly for graph representation? *Advances in neural information processing systems* 34 (2021), 28877–28888.
- [42] Zaixi Zhang, Qi Liu, Qingyong Hu, and Chee-Kong Lee. 2022. Hierarchical graph transformer with adaptive node sampling. *Advances in Neural Information Processing Systems* 35 (2022), 21171–21183.
- [43] Haiteng Zhao, Shuming Ma, Dongdong Zhang, Zhi-Hong Deng, and Furu Wei. 2023. Are more layers beneficial to graph transformers? *The Eleventh International Conference on Learning Representations* (2023).
- [44] Xin Zheng, Yixin Liu, Shirui Pan, Miao Zhang, Di Jin, and Philip S. Yu. 2022. Graph Neural Networks for Graphs with Heterophily: A Survey. *arXiv preprint arXiv:2202.07082* (Feb. 2022).

- [45] Wenhao Zhu, Tianyu Wen, Guojie Song, Xiaojun Ma, and Liang Wang. 2023. Hierarchical transformer for scalable graph learning. In *Proceedings of the Thirty-Second International Joint Conference on Artificial Intelligence*. 4702–4710.
- [46] Wenhao Zhu, Tianyu Wen, Guojie Song, Liang Wang, and Bo Zheng. 2023. On Structural Expressive Power of Graph Transformers. In *Proceedings of the 29th ACM SIGKDD Conference on Knowledge Discovery and Data Mining*. ACM, Long Beach CA USA, 3628–3637. <https://doi.org/10.1145/3580305.3599451>
- [47] Difan Zou, Ziniu Hu, Yewen Wang, Song Jiang, Yizhou Sun, and Quanquan Gu. 2019. Layer-Dependent Importance Sampling for Training Deep and Large Graph Convolutional Networks. In *33rd Advances in Neural Information Processing Systems*.

A ADDITIONAL EXPERIMENTS

A.1 Detailed Experiment Settings

Dataset Details. Table 5 displays the scales and heterophily status of graph datasets utilized in our work. Undirected edges twice in the table. CHAMELEON and SQUIRREL are the filtered version from [28], while OGBN-MAG is the homogeneous variant. We employ 60/20/20 random data splitting percentages for training, validation, and testing sets, respectively, except for OGBN-MAG, where the original split is used. Regarding efficacy metrics, ROC AUC is used on TOLOKERS following the original settings, and accuracy is used for the rest.

Hyperparameters. Parameters regarding the precomputation stage for graph structures are discussed in Section 6.3. For subgraph sampling, we perform parameter search for relative ratio of in/out neighbors represented by s_{out} in range [0, 32]. For sampling weights r_{in}, r_{out} , we search their values in range [-4, 4].

For network architectural hyperparameters, we use $L = 4$ Transformer layers with $N_H = 8$ heads and $F = 128$ hidden dimension for our DHIL-GT model across all experiments. The dropout rates for inputs (features and bias) and intermediate representation are 0.1

and 0.5, respectively. The AdamW optimizer is used with a learning rate of 10^{-4} . The model is trained with 500 epochs with early stopping. Since baseline GTs employ different batching strategies, it is difficult to unify the batch size across all models. We set the batch size to the largest value in the available range without incurring out of memory exception on our 24GB GPU, intending for a fair efficiency evaluation considering both learning speed and space.

Table 5: Statistics of graph datasets. f and N_c are the numbers of input attributes and label classes, respectively. “Train” is the portion of training set w.r.t. labeled nodes.

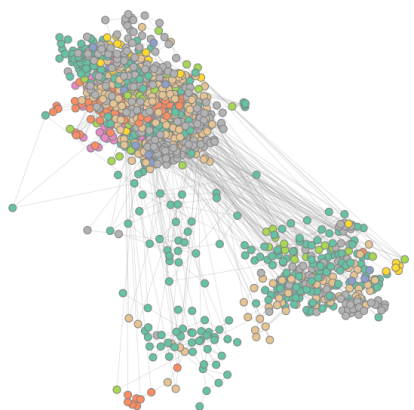
Hetero.	Dataset	Nodes n	Edges m	F	N_c	Train
Homo.	CHAMELEON	890	17,708	2325	5	60%
	SQUIRREL	2,223	93,996	2089	5	60%
	TOLOKERS	11,758	1,038,000	10	2	60%
	PENN94	41,554	2,724,458	4814	2	60%
	GENIUS	421,961	1,845,736	12	2	60%
	TWITCH-GAMER	168,114	13,595,114	7	2	60%
Hetero.	CORA	2,708	10,556	1433	7	60%
	CITeseer	3,279	9,104	3703	6	60%
	PUBMED	19,717	88,648	500	3	60%
	PHYSICS	34,493	495,924	8415	5	60%
	OGBN-ARXIV	169,343	2,315,598	128	40	54%
	OGBN-MAG	736,389	10,792,672	128	349	85%

Received 20 February 2007; revised 12 March 2009; accepted 5 June 2009

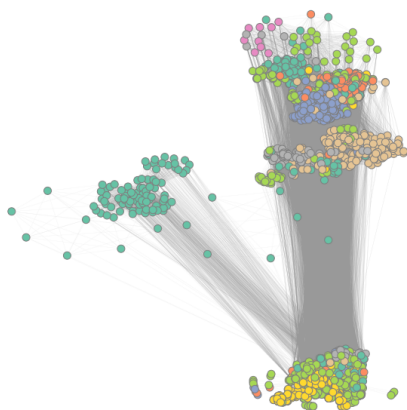
Table 4: Effectiveness and efficiency results on homophilous datasets. “Pre.”, “Epoch”, and “Infer” are precomputation, training epoch, and inference time (in seconds), respectively. “Mem.” refers to peak GPU memory throughout the whole learning process (GB). “OOM” stands for out of memory error. Respective results of the first and second best performances on each dataset are marked in bold and underlined fonts.

Small	CORA					CITeseer					PUBMED				
	Pre.	Epoch	Infer	Mem.	Acc	Pre.	Epoch	Infer	Mem.	Acc	Pre.	Epoch	Infer	Mem.	Acc
DIFFormer*	-	0.11	0.13	1.2	83.37±0.50	-	0.07	0.07	1.7	<u>74.65±0.67</u>	-	0.37	0.35	2.7	75.77±0.40
PolyNormer*	-	0.11	0.65	1.4	80.43±1.55	-	0.21	0.86	1.6	68.70±0.95	-	0.86	6.07	2.5	75.80±0.46
NAGphormer	0.68	0.01	0.06	0.5	76.96±0.73	1.26	0.01	0.38	0.5	62.26±2.10	3.05	0.01	0.04	0.5	78.46±1.01
ANS-GT	43	2.0	1.12	2.0	85.42±0.52	59.9	11.65	4.25	11.9	73.58±0.98	529	14	3.52	1.9	<u>89.53±0.51</u>
GOAT	10.1	0.25	0.93	2.5	78.26±0.17	11.1	0.31	1.04	2.1	64.69±0.43	57.4	0.34	1.61	5.3	77.76±0.97
HSGT*	0.1	1.81	2.33	0.5	81.73±1.95	0.06	0.87	1.23	0.9	69.72±1.02	5.0	3.89	4.44	24	88.86±0.46
DHIL-GT (ours)	0.42	0.05	0.005	10.1	85.58±0.18	0.43	0.05	0.006	9.6	74.91±0.64	2.6	0.25	0.05	9.4	89.80±0.48
Large	PHYSICS					OGBN-ARXIV					OGBN-MAG				
	Pre.	Epoch	Infer	Mem.	Acc	Pre.	Epoch	Infer	Mem.	Acc	Pre.	Epoch	Infer	Mem.	Acc
DIFFormer*	-	1.73	3.79	3.3	96.10±0.11	-	0.89	4.1	2.3	55.90±8.23	-	1.72	9.71	4.2	31.13±0.48
PolyNormer*	-	0.76	2.44	4.1	96.59±0.16	-	0.83	11	7.2	73.24±0.13	-	20	992	22.3	32.42±0.15
NAGphormer	33	8.43	2.43	1.1	<u>96.52±0.24</u>	18	4.36	0.79	2.3	67.85±0.17	89	10.3	2.21	3.8	33.23±0.06
ANS-GT	2203	63.1	34.6	12.5	96.31±0.28	16205	109	2.72	11.3	71.06±0.48	-	-	-	OOM	-
GOAT	45	13.7	12.2	8.7	96.24±0.15	1823	48	61	6.5	69.66±0.73	2673	116	102	6.1	27.69±1.32
HSGT*	12	40.7	61.5	5.0	96.05±0.50	16	475	142	0.3	68.30±0.32	182	582	629	12.6	<u>33.51±1.15</u>
DHIL-GT (ours)	17	0.48	0.03	13.3	96.31±0.42	64	2.02	0.18	5.5	<u>69.17±0.33</u>	7739	14.5	0.16	6.7	33.74±0.24

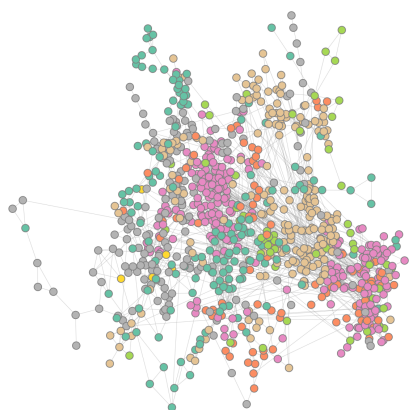
* Inference of these models is performed on the CPU in a full-batch manner due to their requirement of the whole graph.



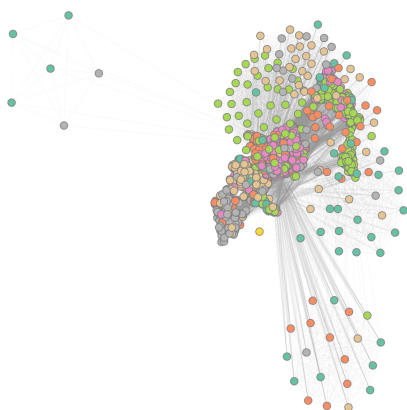
(a) CORA Raw Graph



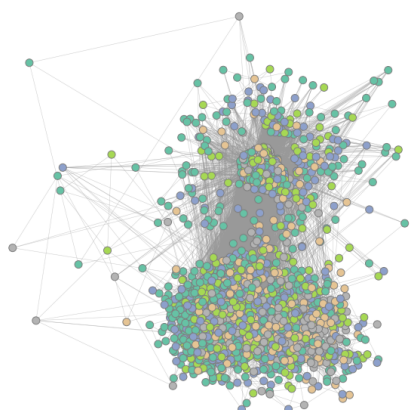
(b) CORA Label Graph



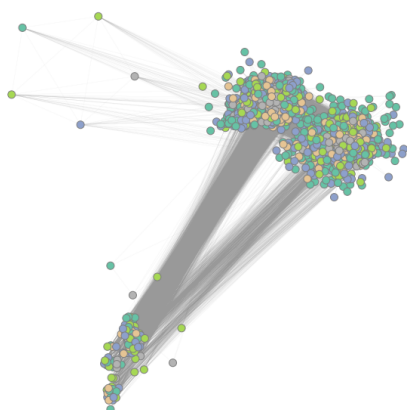
(c) CITESEER Raw Graph



(d) CITESEER Label Graph



(e) SQUIRREL Raw Graph



(f) SQUIRREL Label Graph

Figure 5: Visualization of the hierarchy of original and label graphs on realistic datasets. Color of each node denotes its class.